Journal of Power Sources 196 (2011) 6488–6492

Contents lists available at ScienceDirect

Journal of Power Sources

journal homepage: www.elsevier.com/locate/jpowsour

Short communication

High rate capabilities of all-solid-state lithium secondary batteries using $Li_4Ti_5O_{12}$-coated $LiNi_{0.8}Co_{0.15}Al_{0.05}O_2$ and a sulfide-based solid electrolyte

Yoshikatsu Seino [a,*], Tsuyoshi Ota [a], Kazunori Takada [b]

[a] Idemitsu Kosan Co. Ltd., Kami-izumi 1280, Sodegaura, Chiba 299-0293, Japan
[b] International Center for Materials Nanoarchitectonica, National Institute for Materials, Namiki 1-1, Tsukuba, Ibaraki 305-0044, Japan

ARTICLE INFO

Article history:
Received 4 January 2011
Received in revised form 9 March 2011
Accepted 29 March 2011
Available online 5 April 2011

Keywords:
Lithium battery
Solid electrolyte
Buffer layer
Lithium nickel oxide
Sulfide
Solid state battery

ABSTRACT

Rate capability of $LiNi_{0.8}Co_{0.15}Al_{0.05}O_2$ in solid-state cells was investigated with $70Li_2S$-$30P_2S_5$ glass-ceramics as a sulfide solid electrolyte. It showed higher rate capability than $LiCoO_2$; discharge capacity observed at a current density of 10 mA cm^{-2} was ca. 70 mAh g^{-1}. Surface coating with $Li_4Ti_5O_{12}$ onto the $LiNi_{0.8}Co_{0.15}Al_{0.05}O_2$ particles further improved the high-rate performance to give ca. 110 mAh g^{-1}. The rate capability promises to realize all-solid-state lithium secondary batteries with very high performance.

1. Introduction

Recently, fuel-efficient hybrid-electric and electric vehicles (HEVs and EVs, respectively) have attracted considerable attention due to remarkable increases in fuel costs and increasing environmental concerns. However, there is a strong need to improve their safety, such as by reducing the combustibility of the large secondary batteries equipped in these cars. All-solid-state lithium ion secondary batteries with inorganic solid electrolytes may provide a solution to this problem. However, the power density of solid-state lithium batteries was too low for practical application, even when using highly-conductive sulfide solid electrolytes with an ionic conductivity over 10^{-3} S cm^{-1} [1,2].

Recently, it was found that, when sulfide solid electrolytes are used, the interface between the electrolyte and the oxide cathode determines the performance of all-solid-state lithium batteries. Since the high interfacial resistance was considered to come from highly developed space-charge layer, a thin buffer layer of an oxide solid electrolyte was interposed between the cathode material and the sulfide solid electrolytes in order to suppress the development of the space-charge layer, which was found to reduce the interfacial resistance and improve the battery performance [3–5]. In the studies, the surface of the $LiCoO_2$ particles was covered with a thin film buffer layer of, for example, $Li_4Ti_5O_{12}$ by spray-coating in order to prevent the direct contact. The buffer layer improved their high-rate capability of all-solid-state lithium batteries to be high enough for practical use.

On the other hand, the reduction of cost will be more critical in large batteries. Ni based cathode materials are regarded as one of the candidates because of their lower cost compared to $LiCoO_2$ cathodes. In this study, $LiNi_{0.8}Co_{0.15}Al_{0.05}O_2$ was used as the Ni-based cathode, which are applicable for use in electric vehicle batteries [6,7], and effect of the $Li_4Ti_5O_{12}$ buffer layer on the high rate capability was investigated.

2. Experimental

2.1. Preparation of $Li_4Ti_5O_{12}$-coated $LiNi_{0.8}Co_{0.15}Al_{0.05}O_2$

Commercial $LiNi_{0.8}Co_{0.15}Al_{0.05}O_2$ powder (Toda Kogyo; average particle size of 6.1 μm and Brunauer–Emmett–Teller (BET) surface area of 0.41 m^2 g^{-1}) was used as the Ni-based cathode. It was dried at 200 °C in vacuum for 6 h. The $Li_4Ti_5O_{12}$ coating layer was formed from an ethanol solution of alkoxides of lithium and titanium [3]. Under an Ar atmosphere, 4.1 g (0.59 mol) of lithium metal was dissolved in 487 g of dry ethanol and mixed with 208.9 g (0.74 mol) of titanium tetraisopropoxide. The solution was sprayed onto the $LiNi_{0.8}Co_{0.15}Al_{0.05}O_2$ powder (1.5 kg) at a spraying rate of 2 g min^{-1} by a rolling fluidized coating machine (MP-01, Powrex). The coated

* Corresponding author. Tel.: +81 29 860 4317; fax: +81 29 854 9061.
E-mail address: yoshikatsu.seino@si.idemitsu.co.jp (Y. Seino).

0378-7753/$ – see front matter © 2011 Elsevier B.V. All rights reserved.
doi:10.1016/j.jpowsour.2011.03.090

Table 1
Thickness of $Li_4Ti_5O_{12}$ layer calculated from the doses of the alkoxide solution and ICP-AES results.

Sample	1	2	3
Thickness of $Li_4Ti_5O_{12}$ calculated from the doses of the alkoxide solution [nm]	5	7	10
Thickness of $Li_4Ti_5O_{12}$ derived from the ICP-AES results [nm]	4.2	6.9	8.4

Thickness of $Li_4Ti_5O_{12}$ layer by ICP-AES.

Table 2
Cation ratios on the sample surface estimated from XPS. Results for the $LiNi_{0.8}Co_{0.15}Al_{0.05}O_2$ before the surface coating and $Li_4Ti_5O_{12}$-coated ones with 5 nm thickness annealed at different temperatures are listed in the table.

Sample	Cation ratio (at%)			
	[Li]	[Ti]	[Ni]	[Co]
Pristine $LiNi_{0.8}Co_{0.15}Al_{0.05}O_2$	48	ND	46	7
Annealed at 300 °C	41	37	20	2
Annealed at 400 °C	36	27	30	3

samples were finally heated at 300 °C or 400 °C for 30 min under an air flow to obtain $Li_4Ti_5O_{12}$-coated $LiNi_{0.8}Co_{0.15}Al_{0.05}O_2$.

Commercial $LiCoO_2$ powder (Nippon Chemical Industrial; average particle size 5 μm and Brunauer–Emmett–Teller (BET) surface area of 0.43 $m^2\,g^{-1}$) was used as the Co-based cathode for comparison. The samples were dried at 200 °C in vacuum under for 6 h before the cell assembly.

Thickness of the buffer layer was controlled by changing the amounts of sprayed solution. Table 1 lists thickness of the $Li_4Ti_5O_{12}$, in which the weights of $Li_4Ti_5O_{12}$ calculated from the alkoxide solution doses and deduced from the ICP results were converted into the average thickness using the BET surface area of $LiNi_{0.8}Co_{0.15}Al_{0.05}O_2$ and the density of $Li_4Ti_5O_{12}$ derived from the crystallographic data. The average thicknesses of the coating layers were in accordance with the values expected from the amounts of applied solution.

Fig. 1 shows a scanning electron microscope (SEM, JSM6480LA JEOL) image and elemental mapping of the surface of the $LiNi_{0.8}Co_{0.15}Al_{0.05}O_2$ coated with 5 nm-thick $Li_4Ti_5O_{12}$ after the heat treatments at 300 °C obtained by an energy dispersive spectrometer (EDS). Ti was detected over the surface of the $LiNi_{0.8}Co_{0.15}Al_{0.05}O_2$ particles, which indicates the $Li_4Ti_5O_{12}$ layer was uniformly formed over the surface. However, the surface might not be covered completely. Table 2 lists the surface compositions determined by X-ray photoelectron spectroscopy (XPS) for pristine $LiNi_{0.8}Co_{0.15}Al_{0.05}O_2$ and coated $LiNi_{0.8}Co_{0.15}Al_{0.05}O_2$ with 5 nm-thick $Li_4Ti_5O_{12}$ layer after the heat treatments. XPS measurement was performed with ESCA 5400 using monochromatic Mg-Kα radiation ($h\upsilon$ = 1253.6 eV). Considerable amounts of Ni and Co were detected for the samples whose surface was coated with $Li_4Ti_5O_{12}$. They may suggest that part of the surface of the $LiNi_{0.8}Co_{0.15}Al_{0.05}O$ particles was not covered with $Li_4Ti_5O_{12}$. Of course, the heat treatments will promote diffusion of Ni and Co to make them penetrate the $Li_4Ti_5O_{12}$ layer, which should be also detected in the XPS. In fact, larger amounts of Ni and Co were detected for the sample annealed at higher temperature. That is, although it has not been clear whether the Ni and Co were observed through the openings in the buffer layer or they appeared on the $Li_4Ti_5O_{12}$ layer by the diffusion, it can be concluded that the surface coverage is at least 60%, because [Ti]/([Ni] + [Co]) was 0.62 for the sample annealed at 300 °C.

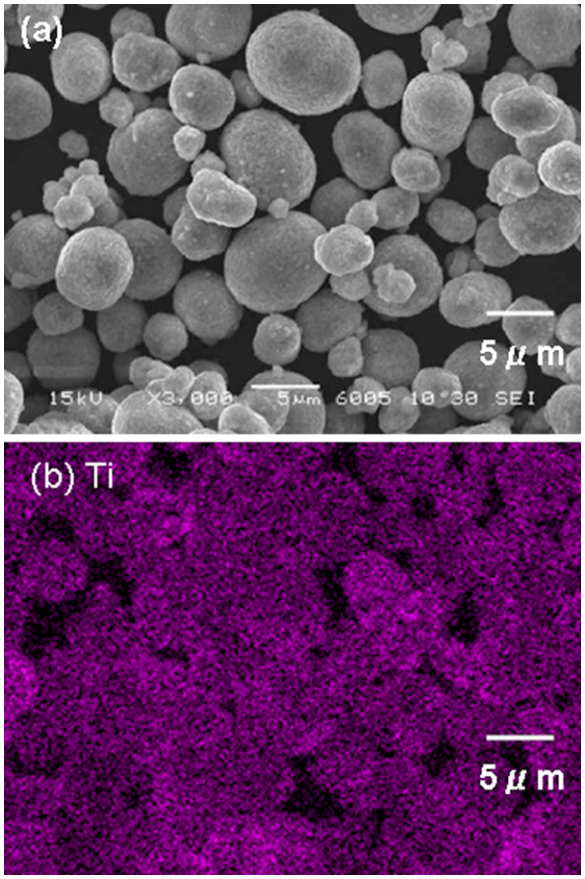

Fig. 1. SEM image (a) and EDS mapping of Ti (b) for $Li_4Ti_5O_{12}$-coated $LiNi_{0.8}Co_{0.15}Al_{0.05}O_2$ particles.

2.2. Electrochemical measurements

Solid state electrochemical cells were fabricated to investigate the high rate capability of the coated $LiNi_{0.8}Co_{0.15}Al_{0.05}O_2$. A glass ceramic with the composition of $70Li_2S$-$30P_2S_5$ was synthesized from reagent-grade P_2S_5 (Aldrich, 99%) and Li_2S (Idemitsu, 99.9%) as the starting materials by the procedure reported in Ref. [8] and was used as the solid electrolytes. Fig. 2 shows a schematic cross-sectional view of a constructed solid state cell. Coated $LiNi_{0.8}Co_{0.15}Al_{0.05}O_2$ was mixed with electrolyte (70/30 in a weight ratio) to form the cathodes, and 15 mg of the mixture was used as the cathode. An indium foil (0.1 mm thick × 10 mmϕ) was used as the anode in the test cells. The indium anode, the solid electrolyte, and the cathode electrode mixture were pressed at 300 MPa into a three-layered pellet with 10 mm in diameter. Stainless steel plates were attached to both sides of the pellet as current collectors to assemble a solid-state cell.

Electrode properties of the $LiNi_{0.8}Co_{0.15}Al_{0.05}O_2$ were investigated by galvanostatic charge–discharge tests and electrochemical impedance spectroscopy (EIS). The charge–discharge tests were

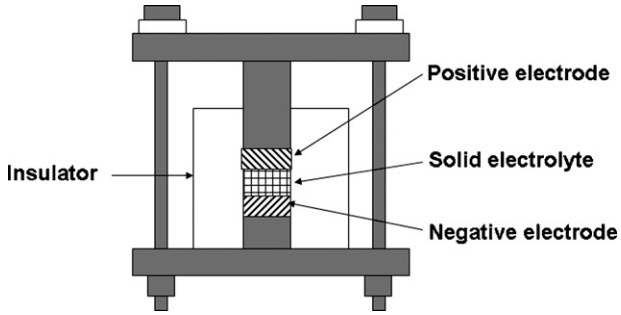

Fig. 2. Cross-sectional view of the battery cell.

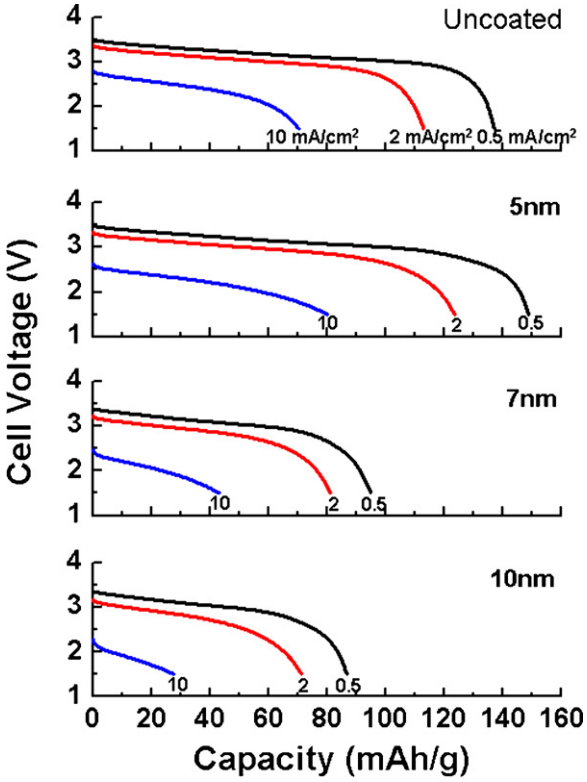

Fig. 3. Discharge curves for $Li_4Ti_5O_{12}$-coated $LiNi_{0.8}Co_{0.15}Al_{0.05}O_2$ heated at 400 °C at various current densities.

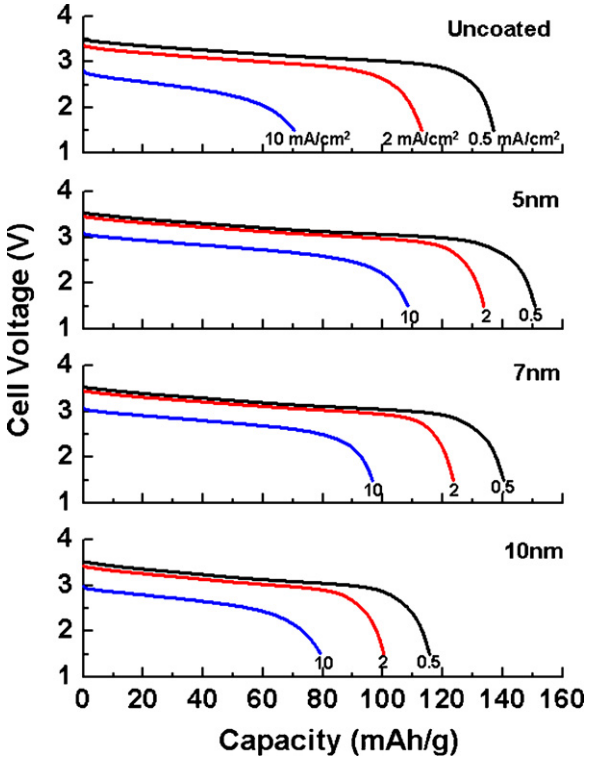

Fig. 4. Discharge curves for $Li_4Ti_5O_{12}$-coated $LiNi_{0.8}Co_{0.15}Al_{0.05}O_2$ heated at 300 °C at various current densities.

performed at room temperature using a multi-channel potentiogalvanostat (PS-08, Tohogiken). The cells were charged to 3.6 V at 0.5 mA cm^{-2} and then discharged to 1.5 V at various current densities. A frequency response analyzer (1260, Solartron Analytical) coupled with an electrochemical interface (1287, Solartron Analytical) was used in the EIS. After the cells were charged to 3.6 V at 0.1 mA cm^{-2}, the impedance spectra were recorded by applying AC perturbation signal of 10 mV with frequency ranging from 10^6 to 10^{-1} Hz.

3. Results and discussion

First, the $Li_4Ti_5O_{12}$-coated $LiNi_{0.8}Co_{0.15}Al_{0.05}O_2$ was prepared by the same procedure as reported in Ref. [3]. That is, after applying the precursor solution of $Li_4Ti_5O_{12}$, the materials were heated at 400 °C for 30 min. The introduction of the $Li_4Ti_5O_{12}$ layer showed the similar tendency to that observed for $LiCoO_2$ in the previous study as shown in Fig. 3. The $Li_4Ti_5O_{12}$ formed with a thickness of 5 nm increased the discharge capacity, and the further increasing thickness decreased it. They can be attributed to the buffer layer effect and the low ionic conductivity of $Li_4Ti_5O_{12}$, respectively [9,10]. However, the improvement was not as drastic as observed in the previous study. One of the conceivable explanations for the difference is fast nickel diffusion into the $Li_4Ti_5O_{12}$ layer.

The previous study on $Li_4Ti_5O_{12}$-coated $LiCoO_2$ system revealed that heat treatment at a higher temperature to decompose the alkoxides and transform them into $Li_4Ti_5O_{12}$ tends to promote cobalt diffusion into the $Li_4Ti_5O_{12}$ layer [5]. Cobalt ions penetrating the $Li_4Ti_5O_{12}$ layer should induce electronic conduction within the layer, and thus the buffer layer could not adequately suppress the development of a space-charge layer to reduce the electrode resistance. Therefore, the heat treatment was performed at relatively low temperature of 400 °C. However, if diffusion of Ni in the $Li_4Ti_5O_{12}$ is faster than that of Co, 400 °C may not be low enough to prevent the inducement of the electronic conduction. When the heat-treatment temperature was decreased to 300 °C, the electrode performance was improved as shown in Fig. 4.

Changes in the high-rate performance for the samples obtained by the heat-treatment of 300 °C were basically the same as that by the heat-treatment of 400 °C: the best performance was observed at the buffer layer thickness of 5 nm, and the further increase of thickness lowered it. However, the achieved performance was considerably higher. For example, the highest capacity observed at 10 mA cm^{-2} among the samples heated at 300 °C was 110 mAh g^{-1}, whereas only 80 mAh g^{-1} was observed for the samples heated at 400 °C. Furthermore, the discharge voltage at 10 mA cm^{-2} was remarkably raised: the starting voltage of the discharge curve increased from 2.5 V to 3.0 V by decreasing the heat-treatment temperature from 400 °C to 300 °C. However, difference between the discharge curves obtained at 10 and 0.5 mA cm^{-2} was still 0.5 V. The voltage drop may be too large for the electrode that can deliver more than 70% of the capacity at the current density. Impedance spectroscopy was performed in order to know which factor is predominant in the voltage drop.

Fig. 5 shows the changes in the electrochemical impedance spectra of the $LiNi_{0.8}Co_{0.15}Al_{0.05}O_2$ by the $Li_4Ti_5O_{12}$ coating. Electrochemical spectroscopy indicated a reduction of the interfacial resistance by the $Li_4Ti_5O_{12}$ coating. Each spectrum consisted of a semicircle in the high-frequency region (>0.5 Hz) and a straight line in the lower-frequency region (>0.5 Hz). Assignment of each response based on a simple Randles circuit is not so easy, because the semicircle was quite distorted. However, comparison of the spectra with that in the previous study [11], suggests that the former and the latter will correspond to the interfacial and Warburg impedances, respectively. On the other hand, the high-frequency limits were nearly constant between 30 and 40 Ω. They should be attributable to the resistance of the electrolyte layer, because they are independent of the electrode and in agreement with that calculated from the conductivity of the solid electrolyte

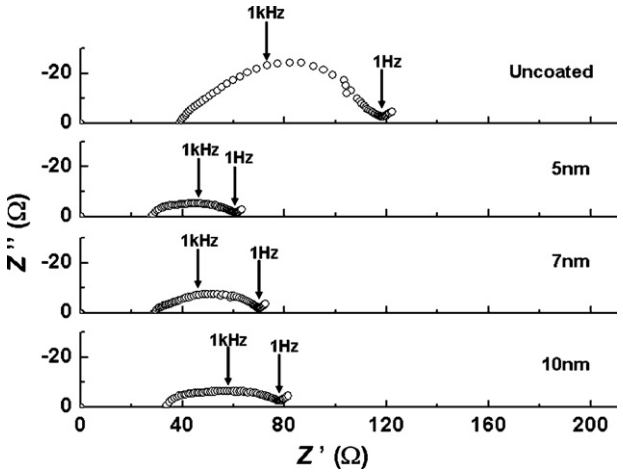

Fig. 5. Complex impedance plots for $Li_4Ti_5O_{12}$-coated $LiNi_{0.8}Co_{0.15}Al_{0.05}O_2$ heated at 300 °C.

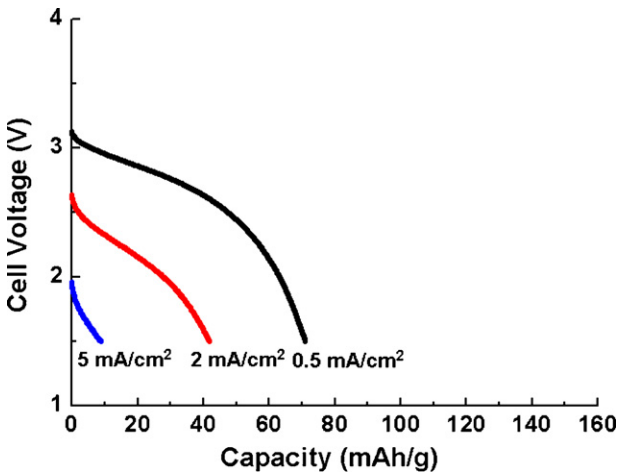

Fig. 7. Discharge curves for uncoated-$LiCoO_2$ with In anode at various current densities.

and the dimensions of the electrolyte layer. It also should be noted that impedance of In–Li electrode was negligible. Fig. 6 shows impedance data of a cell with construction of In–Li/solid electrolytes/In–Li. The interfacial resistance between the In–Li electrode and the solid electrolyte was small enough in comparison with the above two. Therefore, it can be concluded that the impedance of the electrolyte layer is dominant in the battery; 0.3 V out of the voltage drop of 0.5 V observed in the discharge curves should come from the resistance of the electrolyte layer, and the overvoltage related to the electrode reaction will be only 0.2 V.

The high-rate capability observed for $Li_4Ti_5O_{12}$-coated $LiNi_{0.8}Co_{0.15}Al_{0.05}O_2$ in this study was comparable to or somewhat higher than that for $LiCoO_2$ in Ref. [3]. On the other hand, ^7Li NMR study revealed that ionic diffusion in Ni-based cathodes is slower than that in Co-based one [12]. It may suggest that the rate-determining step is not ionic diffusion in the active materials but still in the interface, even after the employment of the buffer layers reduces the interfacial resistance.

In the last of this paper, it should be noted that the $LiNi_{0.8}Co_{0.15}Al_{0.05}O_2$ has a good high-rate capability even without the buffer layer. This study revealed that the improvement of the high-rate capability for $LiNi_{0.8}Co_{0.15}Al_{0.05}O_2$ by the introduction of the $Li_4Ti_5O_{12}$ buffer layer was not as drastic as that for $LiCoO_2$; the buffer layer in Ref. [3] decreased the resistance of $LiCoO_2$ electrode by 1/20, while only by half for the $LiNi_{0.8}Co_{0.15}Al_{0.05}O_2$ electrode as shown in Fig. 5. The reason was the high rate capability of the pristine $LiNi_{0.8}Co_{0.15}Al_{0.05}O_2$; that is, since the pristine material already showed a high power density, the improvement by the $Li_4Ti_5O_{12}$ coating was not remarkable. Of course, different structure of the battery, e.g. composition of the electrode, loading of the active material, can result in different high-rate capability. However, when we investigated the electrode properties of $LiCoO_2$ in the cell with the same structure that used for $LiNi_{0.8}Co_{0.15}Al_{0.05}O_2$, distinguishable difference in the high-rate capability was also found. As shown in Fig. 7, the observed capacity delivered from the $LiCoO_2$ electrode rapidly decreased with increasing discharge current density; only a very small capacity was delivered at 5 mA cm^{-2} discharge, which is in agreement with the results reported in the literature.

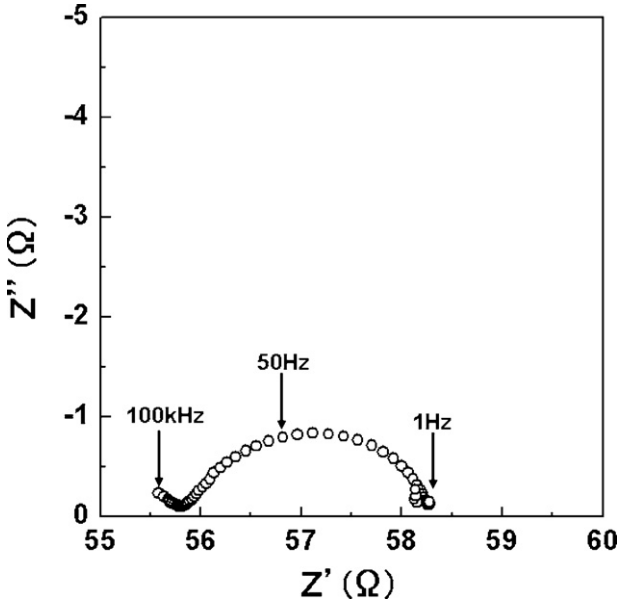

Fig. 6. Complex impedance plots for the In–Li/solid electrolytes/In–Li cell.

The reason for the higher rate capability in the pristine $LiNi_{0.8}Co_{0.15}Al_{0.05}O_2$ than in $LiCoO_2$ has not been clear yet. However, our recent study on $LiCoO_2$ [13] revealed that introduction of Al into $LiCoO_2$ lowers the interfacial impedance and thus enhances the rate capability of $LiCoO_2$ in a sulfide electrolyte. By taking also into account that Ni-based materials have never shown such high rate capability [14,15], it can be speculated that the Al in the pristine $LiNi_{0.8}Co_{0.15}Al_{0.05}O_2$ also plays an important role in the high rate capability.

4. Conclusion

The high rate capability of $LiNi_{0.8}Co_{0.15}Al_{0.05}O_2$ in an all-solid-state lithium battery with a sulfide solid electrolyte was investigated. It showed much better high-rate capability than $LiCoO_2$, and the application of $Li_4Ti_5O_{12}$ buffer layer further enhanced it. We demonstrated the high rate capability of the $Li_4Ti_5O_{12}$-coated $LiNi_{0.8}Co_{0.15}Al_{0.05}O_2$ was high enough to make the power density of all-solid-state lithium-ion batteries comparable to those of commercial lithium ion cells.

References

[1] K. Takada, T. Inada, A. Kajiyama, H. Sasaki, S. Kondo, M. Watanabe, M. Murayama, R. Kanno, Solid State Ionics 158 (2003) 269.
[2] Y. Seino, K. Takada, B.-C. Kim, L.-Q. Zhang, N. Ohta, H. Wada, M. Osada, T. Sasaki, Solid State Ionics 176 (2005) 2389.
[3] N. Ohta, K. Takada, L.-Q. Zhang, R.-Z. Ma, M. Osada, T. Sasaki, Adv. Mater. 18 (2006) 2226.

[4] N. Ohta, K. Takada, I. Sakaguchi, L.-Q. Zhang, R.-Z. Ma, K. Fukuda, M. Osada, T. Sasaki, Electrochem. Commun. 9 (2007) 1486.
[5] K. Takada, N. Ohta, L.-Q. Zhang, K. Fukuda, I. Sakaguchi, R.-Z. Ma, M. Osada, T. Sasaki, Solid State Ionics 179 (2008) 1333.
[6] Y. Itou, Y. Ukyo, J. Power Sources 146 (2005) 39.
[7] H. Kondo, Y. Takeuchi, T. Sasaki, S. Kawauchi, Y. Itou, O. Hiruta, C. Okuda, M. Yoneyama, T. Kamiyama, Y. Ukyo, J. Power Sources 174 (2007) 1131.
[8] F. Mizuno, A. Hayashi, K. Tadanaga, M. Tatsumisago, Adv. Mater. 17 (2005) 918.
[9] S. Takai, M. Kamata, S. Fujine, K. Yoneda, T. Esaka, Solid State Ionics 123 (1999) 165.
[10] S. Hayashi, S. Hatano, J. Ceram. Jpn. 102 (1994) 378.
[11] A. Sakuda, H. Kitaura, A. Hayashi, K. Tadanaga, M. Tatsumisago, Electrochem. Solid-State Lett. 11 (2008) A1.
[12] K. Nakamura, H. Ohno, K. Okamura, Y. Michihiro, I. Nakabayashi, T. Kanashiro, Solid Sate Ionics 135 (2000) 143.
[13] X.X. Xu, K. Takada, K. Watanabe, I. Sakaguchi, K. Akatsuka, B.T. Hang, T. Ohnishi, T. Sasaki, submitted for publication.
[14] K. Takada, N. Aotani, K. Iwamoto, S. Kondo, Solid State Ionics 79 (1995) 284.
[15] N. Machida, H. Maeda, H. Peng, T. Shigematsu, J. Electrochem. Soc. 149 (2002) A688.